0026-895X/08/7304-1113–1121
MOLECULAR PHARMACOLOGY
U.S. Government work not protected by U.S. copyright
Mol Pharmacol 73:1113–1121, 2008

Vol. 73, No. 4
42960/3321326
Printed in U.S.A.

PPP1R16A, The Membrane Subunit of Protein Phosphatase 1β, Signals Nuclear Translocation of the Nuclear Receptor Constitutive Active/Androstane Receptor

Tatsuya Sueyoshi, Rick Moore, Junko Sugatani, Yonehiro Matsumura, and Masahiko Negishi

Pharmacogenetics Section, Laboratory of Reproductive and Developmental Toxicology, National Institute of Environmental Health Sciences, National Institutes of Health, Research Triangle Park, North Carolina

Received October 25, 2007; accepted January 17, 2008

ABSTRACT

Constitutive active/androstane receptor (CAR), a member of the nuclear steroid/thyroid hormone receptor family, activates transcription of numerous hepatic genes upon exposure to therapeutic drugs and environmental pollutants. Sequestered in the cytoplasm, this receptor signals xenobiotic exposure, such as phenobarbital (PB), by translocating into the nucleus. Unlike other hormone receptors, translocation can be triggered indirectly without binding to xenobiotics. We have now identified a membrane-associated subunit of protein phosphatase 1 (PPP1R16A, or abbreviated as R16A) as a novel CAR-binding protein. When CAR and R16A are coexpressed in mouse liver, CAR translocates into the nucleus. Close association of R16A and CAR molecule on liver membrane was shown by fluorescence resonance energy transfer (FRET) analysis using expressed yellow fluorescent protein (YFP)-CAR and CFP-R16A fusion proteins. R16A can form dimer through its middle region, where protein kinase A phosphorylation sites are recently identified. Translocation of CAR by R16A correlates with the ability of R16A to form an intermolecular interaction via the middle region. Moreover, this interaction is enhanced by PB treatment in mouse liver. R16A specifically interacted with PP1β in HepG2 cells despite the highly conserved structure of PP1 family molecules. PP1β activity was inhibited by R16A in vitro and coexpression of PP1β in liver can prevent YFP-CAR translocation into mouse liver. Taken together, R16A at the membrane may mediate the PB signal to initiate CAR nuclear translocation, through a mechanism including its dimerization and inhibition of PP1β activity, providing a novel model for the translocation of nuclear receptors in which direct interaction of ligands and the receptors may not be crucial.

Phenobarbital (PB), a sedative, represents a myriad of therapeutic drugs and environmental chemicals that induce xenobiotic-metabolizing enzymes, such as cytochromes P450. CAR was first identified as a PB-activated receptor mediating the induction of the *CYP2B* genes (Honkakoski et al., 1998; Sueyoshi et al., 1999; Wei et al., 2000). This receptor is now known to be activated, not only by a myriad of xenobiotics but also endobiotics such as estrogens (Kawamoto et al., 2000) and is implicated in the regulation of numerous hepatic genes in xenobiotic, endobiotic, and energy metabolism (Ueda et al., 2002; Kakizaki et al., 2003; Rosenfeld et al., 2003; Kodama et al., 2004; Tien and Negishi, 2006). Furthermore, animal model studies using CAR-null mice revealed that the receptor is an essential factor in chemical promotion of genotoxic carcinogen-induced hepatocellular carcinoma (Yamamoto et al., 2004; Huang et al., 2005) and contributes in pathogenesis of nonalcoholic steatohepatitis (Yamazaki et al., 2007). Although it has become evident that CAR plays an important role in regulating various hepatic functions (Honkakoski et al., 2003; Yamamoto et al., 2003; Qatanani and Moore, 2005; Tien et al., 2007), the molecular mechanism of CAR activation is not yet well understood (Swales and Negishi, 2004; Timsit and Negishi, 2007). Activation seems to begin with the nuclear translocation of CAR, because the receptor, which is retained in the cytoplasm of liver cells, accumulates in the nucleus after treatment with activators such as PB (Kawamoto et al., 1999). Observations

This research was supported by the Intramural Research Program of the National Institutes of Health, National Institute of Environmental Health Sciences.
Article, publication date, and citation information can be found at http://molpharm.aspetjournals.org.
doi:10.1124/mol.107.042960.

ABBREVIATIONS: CAR, constitutive active/androstane receptor; PB, Phenobarbital; FRET, fluorescent resonance energy transfer; YFP, yellow fluorescent protein; CFP, cyan fluorescent protein; R16A, PPP1R16A; PP2A, protein phosphatase 2A; MYPT, myosin phosphatase targeting subunit; PP1, protein phosphatase 1; NR1, nuclear receptor 1; DBD, DNA binding domain; TAP, tandem affinity purification; PKA, protein kinase A; PXR, pregnane X receptor; NE, nuclear extract.

from an experiment directly expressing CAR in mouse livers revealed that CAR contains a LXXLXXL motif (also called Xenobiotic Response Signal) near the C terminus of the molecule that confers xenobiotic responsiveness to the receptor (Zelko et al., 2001). Moreover, the nuclear translocation of CAR occurs in the absence of the ligand-dependent activation function 2. This observation suggests that CAR does not require direct binding of activators for translocation, consistent with the fact that PB and other CAR activators showed no direct binding to the receptor.

Signal transduction is proposed as an alternative mechanism regulating CAR nuclear translocation, because okadaic acid repressed the nuclear accumulation of CAR in PB-treated mouse primary hepatocytes, suggesting the involvement of protein phosphatases (Kawamoto et al., 1999; Yoshinari et al., 2003). CAR forms a protein complex with the 90-kDa heat shock protein and cytoplasmic CAR retention protein in cytoplasm, and PP2A is recruited upon activation by PB (Kobayashi et al., 2003; Yoshinari et al., 2003). To retain CAR in cytoplasm, a signaling pathway including extracellular signal-regulated kinase 1/2 plays an important role (Koike et al., 2007). Furthermore, Ser202 dephosphorylation was reported to be required for mouse CAR translocation into the nucleus (Hosseinpour et al., 2006). In this context, the elucidation of how xenobiotics transmit the signal triggering CAR nuclear translocation is of the highest priority. Using yeast two-hybrid screening, we identified proteins that bound to CAR and found a member of the family of regulatory subunits for serine/threonine protein phosphatase 1 (PPP1R16A or abbreviated as R16A). This mouse protein was originally reported as an interacting protein of PP1 in yeast two-hybrid screening and named MYPT3 (Skinner and Saltiel, 2001) based on its homology with members of the myosin phosphatase targeting subunit (MYPT) family. Although liver is one of multiple mouse tissues that express R16A, hepatic function of R16A is not known.

Here, we first characterized R16A as a membrane-associated protein. Because transformed cells, including HepG2 cells, which are generally used to investigate the translocation mechanism, lack the proper regulation of CAR translocation, fluorescent resonance energy transfer (FRET) and mammalian two hybrid assays were performed directly in mouse livers to investigate the role of R16A in the nuclear translocation of CAR. We here present the experimental consideration that PB elicits signal transduction at the membrane to initiate the translocation of CAR to the nucleus.

Materials and Methods

Animals. Cr1:CD-1(ICR)BR male mice were purchased from Charles River Laboratories, Inc. (Wilmington, MA). For drug treatment, PB (100 mg/kg) was administered i.p. All animal procedures were approved by the Animal Ethics Committee of National Institute of Environmental Health Sciences.

Yeast Two-Hybrid Screening. Matchmaker Gal4 two-hybrid system cDNA library from mouse liver (Clontech, Mountain View, CA) was screened using hCAR L342A/pAS2-1 as bait. We chose to use this mutant as bait for the following reasons: 1, the equivalent mutation in mouse CAR, L352A, abolishes its constitutive transactivation activity (Choi et al., 1997); 2, In its reported three-dimensional structure, the hCAR ligand binding domain formed a complex with RXR and the SRC-1 peptide (Xu et al., 2004), Leu342 exists near the SRC-1 peptide. Based on 1 and 2, we anticipated that the hCAR L342A mutant would have less affinity with the SRC-1 type coactivators. Thus using this mutant may provide less of a chance to reclone coactivators already reported by others in our yeast two-hybrid screening. Four of a total of 53 positive clones from 1.6×10^7 primary transformants matched in sequence with MYPT3/PPP1R16A (Skinner and Saltiel, 2001) (Gene Bank accession number NM_033371).

Plasmids and Antibodies. The plasmids hCAR/pEYFP-c1, hCAR/pECFP-c1 and $(NR1)_5$pGL3-tk were described previously (Kawamoto et al., 1999; Zelko et al., 2001). The following newly constructed plasmids were used in this report. R16A full-length coding cDNA cloned into pCDNA3.1/V5-His TOPO (Invitrogen, Carlsbad, CA); pEYFP-c1 and pECFP-c1 (Clontech); pBind and pAct (Promega, Madison, WI); and pNTAP-B (Stratagene, La Jolla, CA). Human PP1β cDNA cloned into pGEX4T-3 (GE Healthcare, Chalfont St. Giles, Buckinghamshire, UK); pECFP-c1. Human CAR cDNA cloned into pGEX4T-3. All deletion mutants and site directed mutants were constructed using QuikChange site-directed mutagenesis kit (Stratagene) with proper primers. To produce the R16A antiserum, bacterially expressed GST-R16A fusion protein was purified by glutathione-Sepharose (GE Healthcare) and was injected to immunize rabbits. The other antibodies used in this article were: anti-caveolin (BD Transduction Laboratories, San Jose, CA,), anti-tubulin α (Santa Cruz Biotechnology, Santa Cruz, CA), anti-lamin β (Santa Cruz), PP1α (Santa Cruz), anti-PP1β (Santa Cruz), and anti-PP1γ (Santa Cruz).

GST Pull-Down Assay. R16A protein was expressed using the TNT-coupled reticulocyte lysate system (Promega) and pcDNA3.1/R16A. The in vitro-translated ^{35}S-labeled R16A was incubated with GST-hCAR-fusion protein on a glutathione resin at room temperature for 30 min. The resin was washed four times with HEPES-NaOH buffer, pH 7.6, 0.1 M NaCl, 0.1% Triton X-100, and the ^{35}S-labeled R16A bound to the resin was separated on a NuPAGE Novex 4–12% Bis-Tris Gel (Invitrogen) and detected by autoradiography (Kobayashi et al., 2003).

Immunohistochemistry. Frozen mouse liver sections were subjected to immunofluorescent staining using anti-R16A serum (1:100 dilution) and Alexa Fluor 555 goat anti-rabbit IgG (Invitrogen). Fluorescent images of the sections were captured with a confocal Zeiss LSM 510 microscope. Nuclei in the liver sections were stained with Hoechst S33258.

Cell Fractionation and Western Blot. Mouse livers were homogenized in 10 mM HEPES-NaOH buffer, pH 7.6, containing 0.25 M sucrose and complete protease inhibitor cocktail (Roche). The cell membrane fraction was prepared as previously reported (Koike et al., 2005). For cytosolic fraction, the 100,000*g* supernatant of liver homogenates was used. The nuclear extract was prepared as previously reported (Gorski et al., 1986; Honkakoski et al., 1998). For Western blot analysis, proteins were separated on a NuPAGE Novex 4–12% Bis-Tris Gel, and the R16A protein on the PVDF membrane was detected with rabbit anti-R16A serum.

Expression of Fluorescent Protein-Tagged Protein in Liver and Acceptor Photobleaching FRET Analysis. Using the tail vein injection method (Zelko et al., 2001; Sueyoshi et al., 2002), protein was expressed in mouse liver for 8 h with or without PB treatment. Liver frozen sections were prepared, and expressed yellow fluorescent (YFP) and cyan fluorescent (CFP) fusion proteins were visualized under a confocal Zeiss LSM510 microscopy system (Carl Zeiss, Thornwood, NY). For acceptor photobleaching FRET analysis, excited signals (at 458 nm) from 5 μm confocal slices were captured twice before and twice after YFP photobleaching (25 pulses of laser at 514 nm) with a 40× oil immersion objective (1.3 numeric aperture). Emissions of CFP and YFP were collected simultaneously using a META spectral detector (Zeiss) in the range of 450 to 540 nm (Squires et al., 2004). Subsequently, the YFP and CFP emisions were extracted via linear unmixing using software provided by Zeiss. Dequenching of CFP was quantified for multiple liver cells, and FRET efficiency E was calculated with the equation $E = 1 - (Ii/Ii_0)$, where Ii is fluorescence intensity before the bleaching and Ii_0 is that

after the bleaching (Harpur and Bastianens, 2001). Distances between CFP and YFP were estimated from this efficiency E and equation $E = R_0^6/(R_0^6 + R^6)$, where R (nanometers) is the actual distance between the centers of the fluorophores and R_0 (nanometers) is the distance at which energy transfer efficiency E is 50%. R_0 was reported to be 4.9 nm for CFP donor and YFP acceptor combination (Harpur and Bastianens, 2001). A conventional fluorescent microscope (Axioplan; Zeiss, Welwyn Garden City, UK) equipped with specific filter sets for CFP and YFP was employed for counting cell numbers showing differential distribution of YFP-tagged CAR by coexpression of CFP-tagged R16A and its deletion mutants as described in the previous report (Hosseinpour et al., 2006).

Coprecipitation of R16A and PP1β. R16A tagged with tandem affinity peptides was expressed in HepG2 cells plated on 10-cm dish by transfecting the cells with R16A cloned into pNTAP-B (24 μg) using Lipofectamine 2000 (Invitrogen). R16A protein was purified with streptavidin resin (Stratagene) according to the manufacturer's protocol and separated on a SDS-PAGE gel. Two major bands stained with Colloidal Blue Staining Kit (Invitrogen) were subjected to mass spectrometric analysis. Gel bands were excised manually and digested with trypsin (Promega) for 8 h in an automated fashion with a Progest In-gel Digester from Genomics Solutions. Samples were lyophilized to dryness and resuspended in 50:50 (v/v) 0.2% formic acid: acetonitrile. Samples (0.3 μl) were then spotted onto a 192-sample stainless steel MALDI plate and mixed on target with 0.3 μl of 33% saturated α-cyano-hydroxycinnamic acid. Mass spectrometry (MS) and tandem mass spectrometry (MS/MS) were then performed with the use of an Applied Biosystems 4700 Proteomics Analyzer in the positive ion and reflector modes. The MS was calibrated internally using autolytic tryptic peptides, and the MS/MS was calibrated externally using the fragment ions of the angiotensin I M+H ion (*m/z* 1296.68). A focus mass of *m/z* 2000 was used for the MS acquisition. For the MS/MS, 1000 V was used for the collision energy, and argon was used as the collision gas with a recharge threshold set at 1.0×10^{-7} torr. Protein identification was then performed by interrogating both MS and MS/MS using the MASCOT search engine and the entire NCBI nonredundant database. Search parameters included an allowance of two missed tryptic cleavages, a 0.06-Da mass tolerance for the MS data, a 0.1-Da mass tolerance for the MS/MS data, and an allowance for variable oxidation of methionine residues. Western blotting for the same purified materials was performed using anti-PP1α, anti-PP1β, and anti-PP1γ from Santa-Cruz.

Mammalian Two-Hybrid Assay. CheckMate Mammalian Two-Hybrid System (Promega) was used. HepG2 cells were transfected with pG5-Luc, R16A in pBind, and R16A and its deletion mutants in pAct. After 48 h of incubation, firefly luciferase activities from pG5-Luc reporter normalized against *Renilla reniformis* luciferase activities of pBind were determined using the Dual-Luciferase Assay System (Promega, Madison, WI). The same sets of the plasmids were injected via the tail vein using TransIt In Vivo Gene Delivery System (Mirus, Madison, WI). Liver homogenates were prepared in Passive Lysis Buffer (Promega) at 16 h after the DNA injection and luciferase activity was determined.

Phosphatase assay. Protein phosphatase activities of GST-PP1β were assayed using the Protein Serine/Threonine Phosphatase Assay System (New England Biolabs, Ipswich, MA) by following the manufacturer's protocol. Each reaction mixture contains 5 μl of PP1β on the resin and varying amounts of R16A and 10 μM myelin basic protein phosphorylated by PKA and [^{32}P]ATP. After 20-min incubation at 30°C, radioactivity in trichloroacetic acid-soluble supernatant was measured by scintillation counting.

Results

PPP1R16A Interaction with CAR. Yeast two-hybrid screening of a mouse liver cDNA library using human CAR_{L342A}mutant as bait gave us four positive clones along with many RXRα, RXRβ, and corepressors clones. The deduced amino acid sequences of the four positive clones were identical to the previously reported MYPT3, a regulatory subunit of PP1 (Skinner and Saltiel, 2001). MYPT3 has now been classified as PPP1R16A in the mouse genome nomenclature and Entrez Gene database at NCBI (Ceulemans et al., 2002; Cohen, 2002). Hereafter R16A, an abbreviated name of PPP1R16A, will be used. The R16A molecule contains a potential prenylation site at the C terminus, thus indicating that R16A may be a membrane-anchoring protein. In fact, our immunofluorescent staining analysis of liver sections using anti-R16A antibody showed that R16A localized with the cell membrane in mouse livers (Fig. 1A). In Western blot analysis using anti-R16A antibody (Fig. 1B), a band with 70 kDa was detected only in membrane extracted fractions but not in cytosolic or in nuclear extract fractions with or without PB treatment. A GST pull-down assay confirmed that in vitro synthesized R16A bound to GST-CAR but not to GST (Fig. 1*C*). Thus, R16A is a cell membrane-anchoring/targeting subunit of PP1 that can bind to CAR.

R16A Induced CAR Nuclear Translocation. When expressed alone in mouse livers in vivo, CFP-CAR was primarily localized in the cytoplasm and accumulated into the nucleus only after PB induction (Fig. 2A) as previously reported (Zelko et al., 2001; Wang et al., 2004; Xia and Kemper, 2005; Hosseinpour et al., 2006). By injecting expression plasmids via the tail vein, YFP-tagged R16A and CFP-tagged CAR were coexpressed in mouse livers (Fig. 2B). As expected, YFP-R16A was localized to the cell membrane in a similar manner to that observed in Fig. 1A by R16A antiserum. It is noteworthy that cells coexpressing R16A and CAR displayed

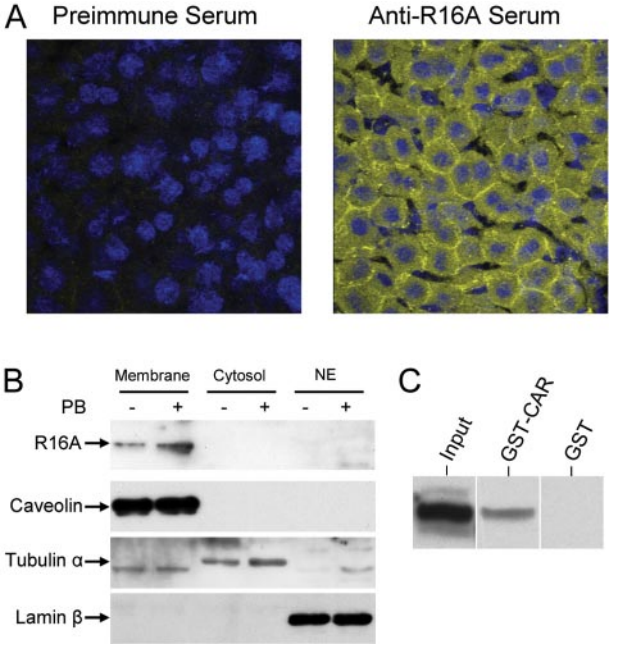

Fig. 1. Membrane localization of R16A and its binding to CAR. A, immunofluorescent staining shows cell membrane localization of R16A. Fluorescence of secondary antibody reacting Anti-R16A and that of nuclear staining was shown in yellow and blue, respectively. B, Western blot detects R16A only in cell membrane fraction. Liver membrane (10 μg/lane), cytosolic (100 μg/lane), and NE (10 μg/lane) fractions were prepared from PB-treated (100 mg/kg for 3 h), and nontreated mice were applied on an SDS polyacrylamide gel, transferred, and stained with anti-R16A antibody. C, GST pull-down assay. The input lane contains 16.7% of GST fusion protein used for pull-down assays.

accumulation of CAR in the nucleus and colocalization of CAR and R16A on the cell membrane. This CAR nuclear localization observed without PB treatment of mice is similar with CAR localization in PB treated mouse liver in Fig. 2A, right, and very different from the localization in control mouse liver in Fig. 2A, left.

R16A Closely Associated with CAR on Liver Membrane. Given the fact that R16A can interact with CAR in yeast cells and the GST pull-down analysis results in Fig. 1C, CAR and R16A may be interacting in the liver in vivo at the colocalization sites on the cell membranes observed in Fig. 2B. To examine this interaction, acceptor photobleaching FRET analysis was performed between YFP-R16A and CFP-CAR using liver cells expressing these two proteins. As illustrated in Fig. 2C, when CFP molecule is excited by a laser at 458 nm, both CFP and YFP fluoresce if these two molecules are close enough to each other so that FRET from CFP to YFP occurs. CFP emission is partially quenched because a part of its excited energy is used to produce YFP emission. After photobleaching YFP (the FRET acceptor molecule in this experimental set up) using 514 nm laser, CFP emission becomes stronger (donor dequenching effect), because there is no energy transfer between the donor and acceptor molecules. The proteins were visualized before and after photobleaching of YFP fusion protein in the area shown with a red square in Figs. 2C and a magnified image of this area was shown in Fig. 2D. The intensity of the CFP-CAR fluorescence in randomly selected areas on the cell membrane (Fig. 2D, area 1–3) increased concomitantly with the decrease of that from YFP-R16A. Quantitative analysis of the CFP-CAR dequenching by YFP-R16A photobleaching was shown in Fig. 2D, bottom. In comparison, CFP-CAR intensity localized in the nuclei was not changed by photobleaching (Fig. 2D, area 4). Similar analysis of YFP and CFP fluorescent intensity on the membranes of more than 10 cells revealed that the FRET efficiency between YFP-16A and CFP-CAR was 61 ± 11%. FRET efficiency E was calculated with the equation $E = 1 - (Ii/Ii_0)$, where Ii is CFP-CAR fluorescence intensity before the bleaching of YFP-R16A and Ii_0 is that of after the bleaching (Harpur and Bastianens, 2001). Using a $R_0 = 4.9$ nm, the distance at which energy transfer efficiency is 50% in ideal conditions for CFP donor and YFP acceptor (Harpur and Bastianens, 2001), the distance between the two tags was estimated to be 4.6 ± 0.36 nm. This distance can be even

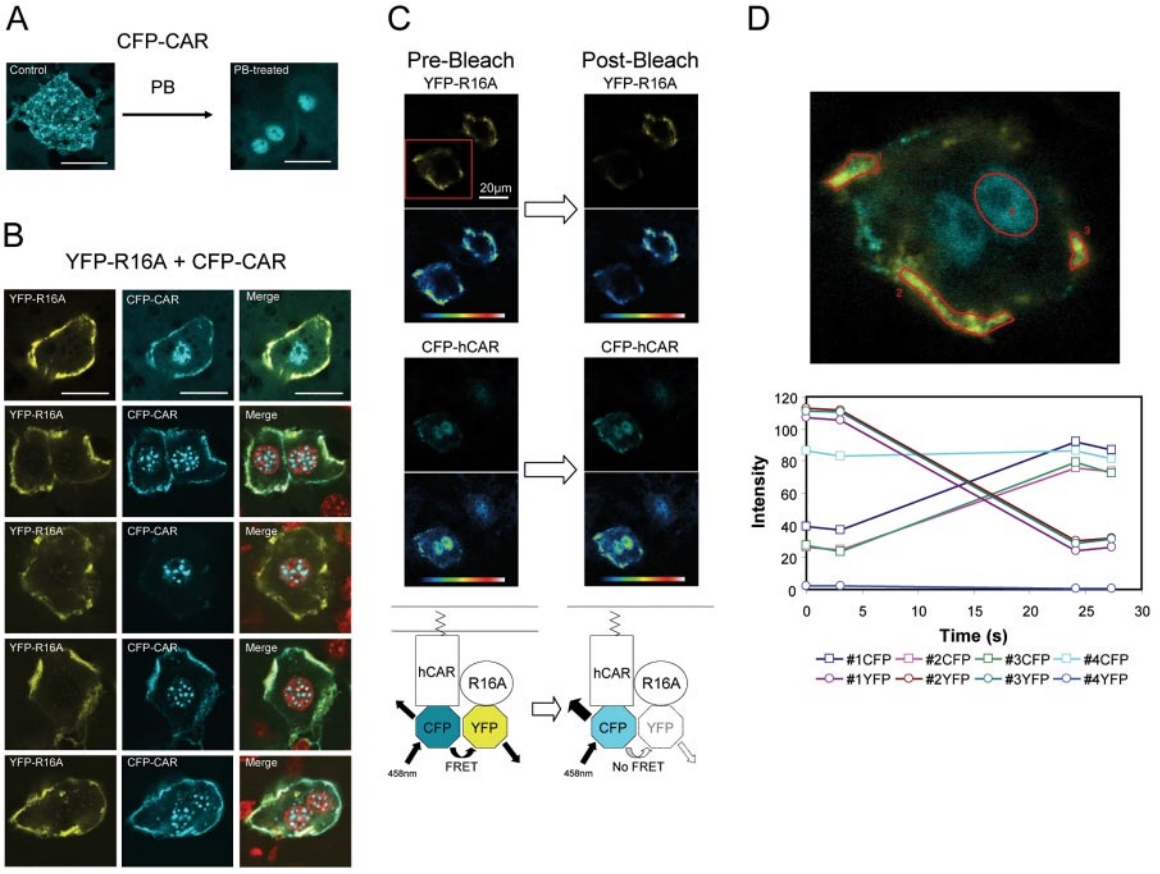

Fig. 2. R16A-mediated nuclear localization of CAR in mouse liver. CFP-hCAR and YFP-R16A fusion proteins were expressed in mouse livers by injecting the expression plasmids via tail vein. A, CFP-hCAR localization in liver section before and after PB treatment. B, CFP-hCAR localization in nucleus by coexpression of YFP-R16A without PB treatment. CFP-hCAR was coexpressed with YFP-R16A in mouse liver, and images for each fusion protein were captured as described under *Materials and Methods*. The three horizontal panels show images from the same microscopic analysis. Red color in merged images shows nuclear staining. White scale bars, 20 μm. C, FRET between CFP-hCAR and YFP-R16A in mouse liver in vivo. Images of CFP-hCAR and YFP-R16A that are expressed in the same liver cells are shown. Each image is presented with two panels: the top is the direct image, and bottom is the color-coding image for fluorescence intensity. Color-coded bars on the bottom indicate the fluorescence intensity, with higher values toward the right. The area of laser irradiation (at 514 nm) for photobleaching YFP is boxed with a red line. D, FRET quantification in selected areas in the photobleached cell. The changes of the fluorescent intensity in four areas shown at the top were monitored before and after photobleaching. Images were captured four times at times 0, 3.1, 24.1, and 27.3 s and plotted as a graph at the bottom. Photobleaching was performed between 3.1 and 24.1 s.

smaller given the fact that FRET can be less effective depending on the orientations of dipoles and the environment of the fluorescent dyes. Although the results do not establish the direct interaction of the two molecules, the results are consistent with the hypothesis that R16A and CAR are directly interacting on the membrane, considering that their estimated radii from molecular weight of these proteins using the equation for globular proteins, $r = 6.76 \times 10^{-2}$ $MW^{1/3}$, are 2.3 and 2.6 nm, respectively.

Dimerization of R16A and CAR Nuclear Translocation. Acceptor photobleaching FRET analysis was applied for YFP-R16A and CFP-R16A coexpressed in mouse liver. YFP-R16A molecule in the area shown with red square was photobleached as in Fig. 3A and a magnified image of the area was shown in Fig. 3B. The intensity of the CFP-R16A fluorescent in randomly selected areas on the cell membrane (Fig. 3B, area 1–4) increased concomitantly with the decrease of that from YFP-R16A. Although relative fluorescence intensities differed in these areas, all areas randomly chosen showed that the intensity of CFP-R16A fluorescence increased as that of YFP-R16A decreased after photobleaching. The similar analysis, using more than 10 liver cells determined, that the FRET efficiency between YFP-16A and CFP-R16A was 31 ± 7% and suggested that two tags connected with R16A molecules were present within an estimated distance of 5.6 ± 0.32 nm, thus indicating the intermolecular interaction of R16A on the cell membrane. A mammalian two-hybrid assay was performed to obtain additional evidence supporting the direct interaction of R16A molecules and to delineate a region of the molecule responsible for this interaction. Luciferase activity from a Gal4 binding site driven reporter was increased when pBind-R16A and pAct-R16A were coexpressed in HepG2 cells (Fig. 4A). The coexpression of the C-terminal subdomain (R16A304–524), but not the N-terminal subdomain (R16A1–303), increased luciferase activity. These results suggest that the C-terminal fragment can mediate the intermolecular interaction of R16A. Subsequently, three deletion mutants within the C-terminal fragment were generated to delineate the region responsible for the intermolecular interaction: R16AΔ304–513, R16AΔ304–403, and R16AΔ404–513 (Fig. 4A). In the mammalian two-hybrid assay, R16AΔ403–513 strongly interacted with R16A, although the degree of the interaction was approximately 60% of the R16A-R16A interaction, whereas R16AΔ304–403 exhibited a weak interaction with R16A and R16AΔ304–513 showed no interaction. Thus, the

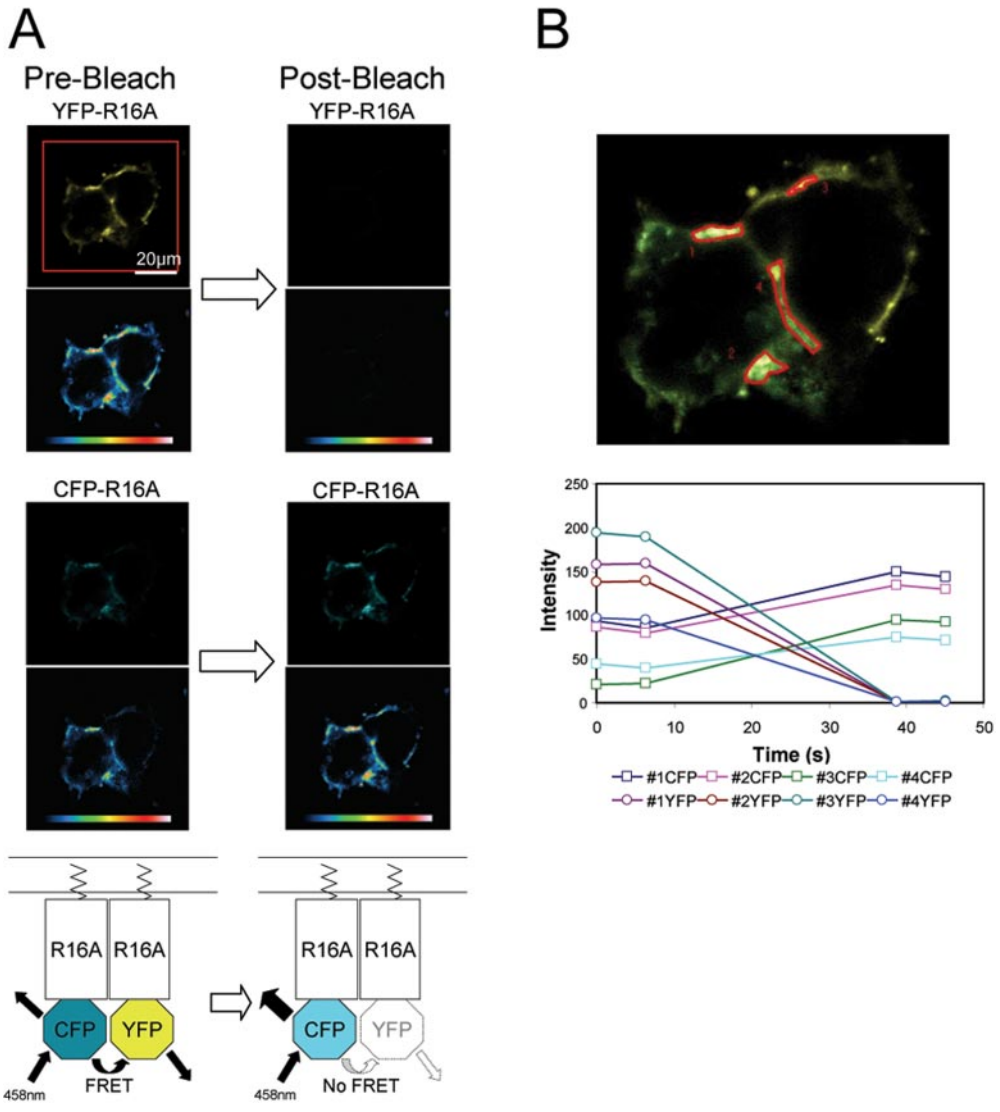

Fig. 3. FRET between CFP-R16A and YFP-R16A in mouse liver in vivo. A, images of CFP-R16A and YFP-R16A that are expressed in the same liver cells. Each image is presented with two panels: the top is the direct image, and bottom is the color-coding image for fluorescence intensity. Color-coded bars at the bottom indicate the fluorescence intensity, with higher values toward the right. The area of laser irradiation (at 514 nm) for photobleaching YFP is boxed with red line. B, FRET quantification in selected areas in the photobleached cells. The changes of the fluorescent intensity in the four areas shown at the top were monitored before and after photobleaching. Images were captured four times at times 0, 6.3, 38.8, and 45.1 s and plotted as a graph in the lower panel; photobleaching was performed between 6.3 and 38.8 s.

intermolecular interaction resides in the middle of the R16A molecule including the 304–403 region.

Next, we examined whether a correlation existed between the CAR translocation capability and intermolecular interaction of R16A. YFP-tagged CAR was directly expressed in mouse livers together with CFP tagged R16A, R16A1–303, R16A304–524, R16AΔ304–513, R16AΔ304–403, or R16AΔ404–513 to analyze its intracellular localization (Fig. 4B). Of more than 100 cells counted, 80% retained CAR in the cytoplasm if it was expressed alone. When CAR was coexpressed with R16A, 70% of cells predominantly localized CAR in the nucleus, and another 10% showed CAR localized equally in the nucleus and cytoplasm. The coexpression of the R16A303–524 greatly increased the number of cells localizing CAR to the nucleus, whereas that number was not increased when the R16A1–303 was coexpressed. With respect to deletion mutants, R16AΔ304–513 did not alter the cytoplasmic localization of CAR. In the case of R16AΔ304–403, a slight decrease of cytoplasmic CAR localization inversely correlated with a similar increase of the receptor in the nucleus, suggesting the weak ability of R16AΔ304–403 to nuclear translocate CAR. The strongest CAR nuclear translocation activity was observed with R16AΔ404–513 (Fig. 4B); nearly 40% decrease in cytosolic localization was replaced by a 30% increase in predominantly nuclear localization. The order of strength of R16A and its deletion mutants in translocation of CAR into the nucleus was: R16A = R16A304–524 > R16AΔ404–513 ≫ R16AΔ304–403 > 16AΔ304–513 = R16A1–303. This order was identical to the strength of the intermolecular interaction of R16A and its mutants as seen in mammalian two-hybrid assay, thus correlating the interaction with the CAR nuclear translocation in mouse livers.

If, in fact, R16A regulates xenobiotic-induced nuclear translocation of CAR, R16A should be able to form the interaction in response to xenobiotics. To obtain evidence for PB-elicited interaction of R16A, a mammalian two-hybrid assay was performed in mouse livers, in which pBind-R16A and pAct-R16A were coinjected into mice via the tail vein and the mice were treated with PB. The livers were removed, homogenized, and subjected to luciferase assay. PB treatment increased luciferase activity by 3-fold, indicating that it enhanced the interaction of R16A molecules (Fig. 5). Likewise, R16A304–524 also increased the interaction with R16A after PB treatment. In contrast, when pBind-R16AΔ304–513, which lacks the region responsible for the interaction, was coinjected with pAct-R16A, PB treatment did not enhance their interaction. In a control experiment, R16A showed no interaction with Gal4 DBD and VP16 activation domain, either before or after PB treatment. In non–PB-treated animals, pBind-R16A and pAct-R16 cotransfection gave 1.5- to 2.0-fold higher reporter activity than that of the two negative controls using R16A expression vectors and empty vectors. The weak basal R16A dimerization in mouse liver nuclei is consistent with the R16A dimerization on the liver cell

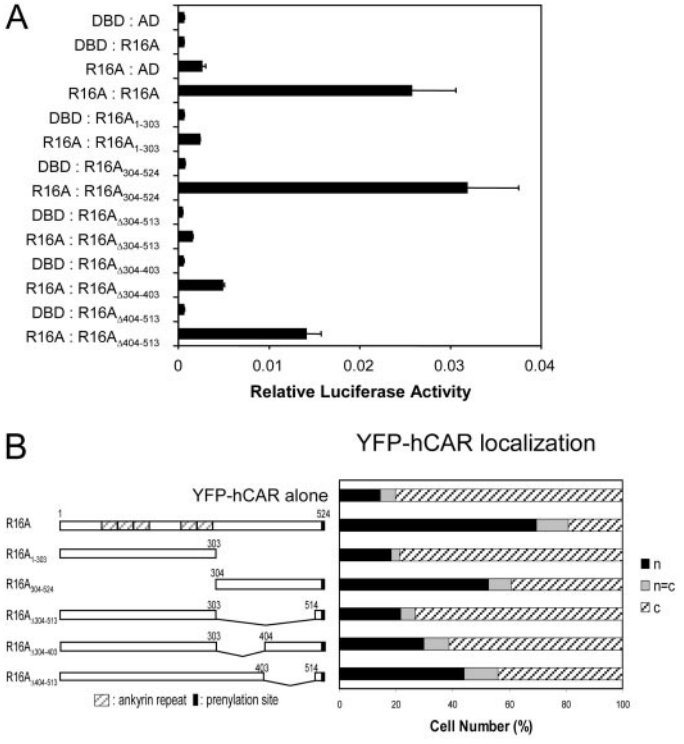

Fig. 4. Intermolecular interaction potency of R16A molecules correlates with potency for CAR nuclear localization. A, R16A intermolecular interaction shown by mammalian two-hybrid assays. The assay was performed using wild-type R16A and various deletion mutants as described under *Materials and Methods*. cDNA encoding a full-length R16A was cloned into pBind, for expression of Gal4 DBD-R16A fusion protein. R16A and deletion mutants were cloned into pAct, for expression of VP16 AD fusion proteins. DBD and AD indicate empty pBind and pAct vectors. Bars indicate the standard deviation from triplicate measurements. B, YFP-hCAR localization in liver cells coexpressing CFP-R16A and its deletion mutants. YFP-hCAR was coexpressed with CFP-R16A or each of the deletion mutants in mouse livers. Top bar shows YFP-hCAR localization without any coexpression. Intracellular localization was categorized into three groups: nuclear localization (N), cytoplasmic localization (C), similar localization in both nucleus and cytoplasm (N = C). Approximately 120 cells were randomly selected for each group to analyze the localizations. Schematic representation of R16A and deletion mutants coexpressed with YFP-hCAR are shown on the left side of the categorized data.

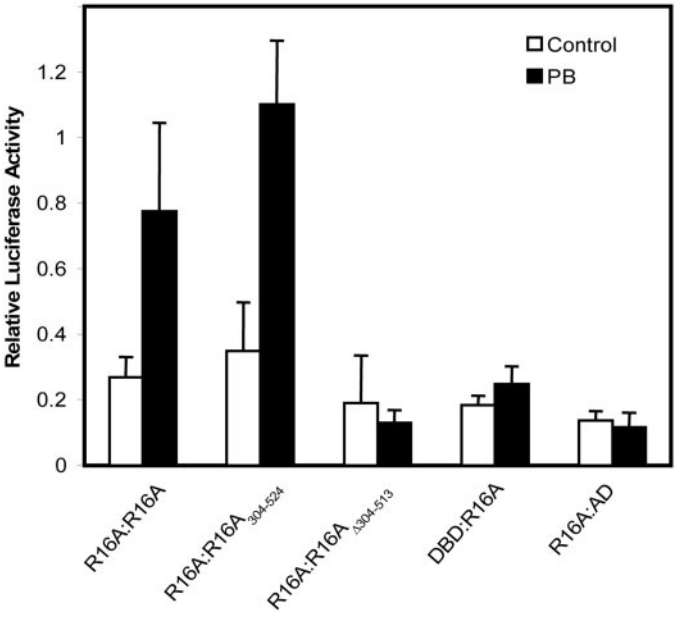

Fig. 5. PB-elicited intermolecular interaction of R16A in mouse liver. Mammalian two-hybrid assay showing increased interaction of R16A in mouse liver after treatment with PB. Plasmids were injected via the tail vein, and mice were treated with PB as described under *Materials and Methods*. DBD and AD represent pBind and pAct used as controls, respectively. Bars indicate means with standard deviation from quadruplicate measurements.

membrane observed by FRET analysis in Fig. 3. The degree of interactions detected by these two methods can not be directly compared because of the very different nature of these two methods. The results indicate that PB can increase the interaction of R16A molecules in mouse liver.

Specific Interaction between R16A and PP1β. Because R16A was originally reported as a PP1-interacting protein (Skinner and Saltiel, 2001), R16A and PP1 interaction was examined in HepG2 cells. Tandem affinity purification (TAP) tagged R16A was expressed in HepG2 cells and precipitated with streptavidin resin. Then the precipitated materials were separated on an SDS-PAGE gel, and two major proteins were detected by Coomassie Brilliant Blue staining. Mass spectrometry analysis identified the two bands as R16A and human PP1β catalytic subunit (data not shown). Because there are highly homologous subtypes of PP1 catalytic subunit in HepG2 cells, we analyzed the same samples further using specific antibodies against PP1 subtypes. TAP-R16A was shown to be efficiently precipitated by streptavidin resin as detected by Western blotting using anti-R16A serum (Fig. 6A). In crude extracts, in addition to ectopically expressed TAP-tagged R16A, human R16A in HepG2 cells were detected by our antibody. Endogenous R16A was copurified, possibly because of dimer formation of R16A molecules, in the eluent from streptavidin resin. Using anti PP1 antibodies, only PP1β-specific antibody detected a band in streptavidin resin purified fraction, whereas anti-PP1α or anti-PP1γ antibodies did not. The results overall established specific interaction of PP1β and R16A. Next we analyzed PP1β activity modulation by R16A. PP1β activity was effectively inhibited (more than 60%) by R16A protein expressed in bacteria as GST fusion protein (Fig. 6B). We also analyzed the inhibition by mutant R16A (F67A and F69A double mutation), which has a mutated PP1 interaction consensus sequence identified in a previous report (Skinner and Saltiel, 2001). The mutant was around 30% less effective at inhibiting PP1β, suggesting existence of secondary interaction sites in R16A for PP1β inhibition. In contrast with these fusion proteins, GST alone had no effect on the protein phosphatase activity.

PP1β Inhibited CAR Translocation by PB. To analyze PP1β effect on PB-induced CAR nuclear translocation, CFP-tagged PP1β was coexpressed in liver cells with YFP-tagged CAR, and the CAR localization change by PB was analyzed. As reported previously (Zelko et al., 2001; Hosseinpour et al., 2006), without PB, less than 20% of the cells show exclusively nuclear YFP-hCAR localization, and PB treatment increased this value to nearly 70%. Active PP1β coexpression increased CAR nuclear localization slightly without drug treatment. With PB, however, YFP-hCAR translocation into nucleus was strongly inhibited by the coexpression (Fig. 7A). In contrast, mutated PP1β, in which the active center histidine was replaced by alanine ($PP1\beta_{H124A}$), has no effect on translocation. To evaluate the effect of PP1β inhibition of CAR nuclear translocation against the receptor's transactivation activity, we next examined CAR activity in the liver using a NR1 reporter gene (Fig. 7B). The NR1 reporter has been well established to be activated by CAR (Kawamoto et al., 1999; Sueyoshi et al., 1999). Mouse livers were transfected with $(NR1)_5$pGL3-tk reporter with PP1β or its active site mutant. The reporter was activated by PB at approximately 3.5-fold. This activation was strongly inhibited by active PP1β coexpression, and the no PB activation was observed. Meanwhile, PP1β active site mutant H124A showed no effect on reporter activation by PB treatment. Thus, these results were consistent with PP1β's effect on CAR translocation.

Discussion

In this article, the role of R16A, a membrane-anchored subunit of PP1, in regulating CAR nuclear translocation was investigated in mouse liver. Direct interaction between R16A and CAR was suggested by in vitro and in vivo experiments including FRET analysis in liver cells. R16A coexpression induced CAR translocation into the nucleus. R16A seems to be capable of forming intermolecular interaction in response to PB, and potency for the dimer/oligomer formation and

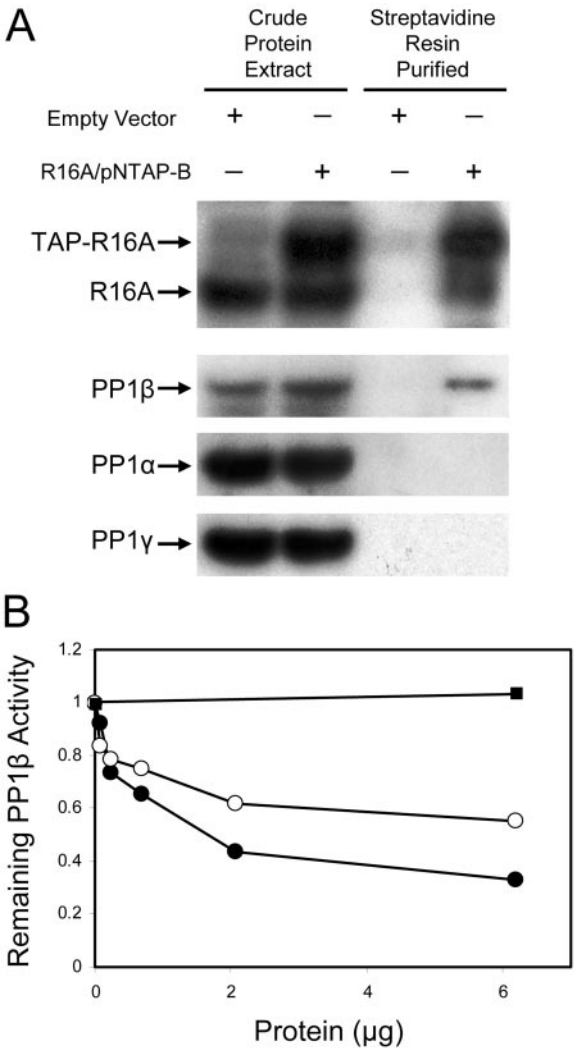

Fig. 6. R16A specifically interacts with PP1β. A, tandem affinity tagged R16A (TAP-R16A) was expressed in HepG2 cells by transfecting the cells with R16A/pNTAP-B plasmid. Tagged R16A was purified by Streptavidin resin as under *Materials and Methods*. Crude and purified materials were separated on a SDS-PAGE gel and Western blotting was performed with anti-R16A, anti-PP1β, anti-PP1α, and anti-PP1γ antibodies. B, R16A inhibition of PP1β activity. PP1β activities were determined with varying amounts of GST-R16A (●), PP1 binding consensus mutant form of GST-R16A (○) or GST (■) using ^{32}P-labeled myelin basic protein as substrate as described under *Materials and Methods*. Relative remaining activities were calculated taking PP1β activity without adding inhibitors as one unit.

induction of nuclear translocation seems to be correlated. Furthermore, R16A specifically interacts with PP1β and inhibits its activity, whereas active PP1β in liver cells is inhibitory for nuclear translocation of CAR. Although many questions remain unanswered at this point, R16A may provide a clue for understanding the signaling mechanism that can regulate the nuclear translocation and activation of CAR. In this mechanism, CAR might exist on the cell membrane before moving into the nucleus by drug activation. In fact, a recent report (Koike et al., 2005) found CAR exists on the cell membrane. At the cell membrane, a R16A dimer/oligomer, which is induced by an unidentified signal originated from the drug activation, and CAR may form a temporal complex while CAR is activated to translocate into the nucleus. Our FRET analysis has demonstrated the close interactions of CAR with R16A on the cell membrane, supporting the notion that formation of this temporal complex can occur in the liver cell. Coprecipitation of endogenous CAR and R16A from the detergent-soluble fraction of the cell membrane using their antibodies did not allow us to detect a complex of these two proteins. In addition to several experimental difficulties, such as low contents of these proteins in the membrane fractions and the qualities of the antibodies currently available to us, the possible temporal and weak nature of their interactions may have prevented us from detecting an endogenous CAR-R16A complex. In the CAR activation process in the complex, the PP1β activity modulation by R16A may be involved. CAR translocation caused by R16A over expression without PB treatment may be triggered by spontaneous dimer/oligomer formation of R16A on the liver cells membrane. Even partial R16A, which lacked a PP1 binding consensus (residues 304–524), showed strong activity for CAR translocation (Fig. 6B). Dimer/oligomer formed between this deletion mutant and the endogenous R16A in mouse liver may be contributing the activity we observed.

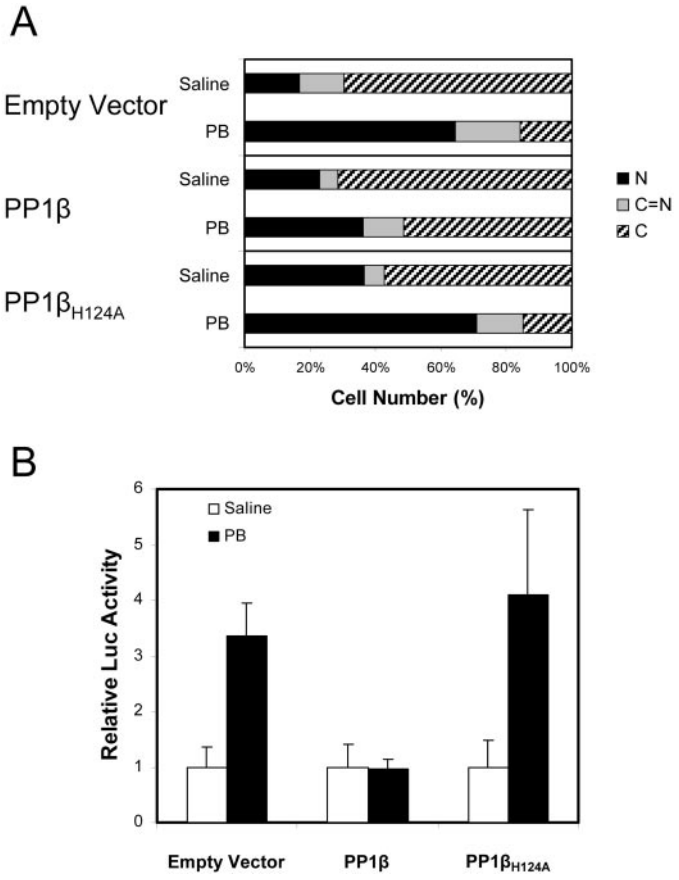

Fig. 7. PP1β inhibits nuclear translocation of CAR. A, CFP-hCAR was coexpressed in mouse liver with YFP-tagged PP1β, its active site mutant PP1β_{H124A} or YFP alone. Mice are treated with PB and liver sections were analyzed under microscope. Intracellular localization was categorized into three groups: nuclear localization (N), cytoplasmic localization (C), similar localization in both nucleus and cytoplasm (N = C). Approximately 120 cells were randomly selected for each group to analyze the localizations. B, inhibition of PB induced NR1 reporter activities by coexpression of PP1β in mouse liver. NR1 luciferase reporter plasmid was coinjected into mice with PP1β, its active site mutant (PP1βH$_{124A}$), or empty expression plasmids through tail vein. Luciferase activities in livers from PB or saline-treated mice were determined as under *Materials and Methods*. Bars indicate means with standard deviation from quadruplicate measurements.

R16A was originally identified as a PP1α catalytic subunit interacting protein (Skinner and Saltiel, 2001) in yeast two hybrid screening and named MYPT3 based on the similarity with MYPT proteins. R16A consists of 524 amino acid residues, in which five Ankyrin repeats and a consensus PP1 binding site are located within the N-terminal 300 amino acid residues. The C-terminal region with 224 residues contains two possible Src homology 3 binding sites and a prenylation motif (CaaX). These structural features suggest that R16A could be a scaffold protein regulating protein-protein interactions as well as cellular signaling. Our results demonstrated membrane localization of this protein. Furthermore, deletion mutants that retain the CaaX motif were distributed on the membrane, but deletion mutants that lacked this motif were not (data not shown) suggesting that the CaaX motif is in fact farnesylated to localize the molecules on the cell membrane in liver. R16A shows a highly specific interaction with PP1β, which is one of the three PP1 catalytic subunits in humans, PP1α, PP1β (also called PP1δ), and PP1γ. These are extremely homologous proteins, with 88% amino acid identity between PP1β and PP1α and 87% between PP1β and PP1γ. Consistent with our results, similar specific interaction between R16A and PP1β has been reported quite recently using His-tagged R16A expressed in COS-7 cells (Yong et al., 2006). In *Drosophila melanogaster*, orthologous proteins of mammalian R16A and PP1β specifically interact with each other (Vereshchagina et al., 2004). From these facts, we postulated that PP1β might have effects on CAR nuclear translocation and NR1 reporter activation. Indeed, as shown in Fig. 4, PP1β activity was inhibitory for the translocation and activation of the reporter. A recent report established that PKA phosphorylation of R16A could affect inhibitory activity for PP1β (Yong et al., 2006). Upon PKA phosphorylation, R16A intermolecular interactions were significantly reduced, and it became an activator for PP1β. Furthermore, suggested phosphorylation sites are localized in the region that is critical for dimerization (Ser340, Ser341, and Ser353 in human R16A). Thus, how PKA regulates R16A dimerization for PP1β activity modulation in PB induced CAR translocation and activation is an area for further study.

Collectively, R16A widens our insight into understanding the induction mechanism by xenobiotics and may lead us one step closer to the initial site of PB action. An increasing number of CAR activators such as phenytoin are now included with those displaying the same activation characteristics as PB (Jackson et al., 2004; Wang et al., 2004). The

other xenosensing nuclear receptor PXR has also been reported to translocate into the nucleus in response to an activator (Kawana et al., 2003; Squires et al., 2004), and preliminary results suggested this receptor also interacts with R16A (data not shown). Because PXR and CAR are activated by numerous xenobiotics, including therapeutic drugs and environmental pollutants, affecting drug toxicity and drug-drug interactions (Honkakoski and Negishi, 2000; Xie and Evans, 2001; Willson and Kliewer, 2002; Honkakoski et al., 2003), R16A may provide us with a novel candidate as target of the xenobiotics that can modulate the function of these receptors.

Acknowledgments

We thank Jeff Reece and Jason Williams, at the National Institute of Environmental Health Sciences fluorescent microscopy and protein microcharacterization core facilities, respectively, for technical assistance.

References

Ceulemans H, Stalmans W, and Bollen M (2002) Regulator-driven functional diversification of protein phosphatase-1 in eukaryotic evolution. *Bioessays* **24:**371–381.
Choi HS, Chung M, Tzameli I, Simha D, Lee YK, Seol W, and Moore DD (1997) Differential transactivation by two isoforms of the orphan nuclear hormone receptor CAR. *J Biol Chem* **272:**23565–23571.
Cohen PT (2002) Protein phosphatase 1–targeted in many directions. *J Cell Sci* **115:**241–256.
Gorski K, Carneiro M, and Schibler U (1986) Tissue-specific in vitro transcription from the mouse albumin promoter. *Cell* **47:**767–776.
Harpur AG and Bastianens PIH (2001) Probing protein interactions using GFP and fluoresence resonance energy transfer, in *Molecular Cloning A Laboratory Manual* (Sambrook J and Russell DW eds) pp 18.69–18.96, Cold Spring Harbor Laboratory Press, Cold Spring Harbor, NY.
Honkakoski P and Negishi M (2000) Regulation of cytochrome P450 (CYP) genes by nuclear receptors. *Biochem J* **347:**321–337.
Honkakoski P, Sueyoshi T, and Negishi M (2003) Drug-activated nuclear receptors CAR and PXR. *Ann Med* **35:**172–182.
Honkakoski P, Zelko I, Sueyoshi T, and Negishi M (1998) The nuclear orphan receptor CAR-retinoid X receptor heterodimer activates the phenobarbital-responsive enhancer module of the CYP2B gene. *Mol Cell Biol* **18:**5652–5658.
Hosseinpour F, Moore R, Negishi M, and Sueyoshi T (2006) Serine 202 regulates the nuclear translocation of constitutive active/androstane receptor. *Mol Pharmacol* **69:**1095–1102.
Huang W, Zhang J, Washington M, Liu J, Parant JM, Lozano G, and Moore DD (2005) Xenobiotic stress induces hepatomegaly and liver tumors via the nuclear receptor constitutive androstane receptor. *Mol Endocrinol* **19:**1646–1653.
Jackson JP, Ferguson SS, Moore R, Negishi M, and Goldstein JA (2004) The constitutive active/androstane receptor regulates phenytoin induction of Cyp2c29. *Mol Pharmacol* **65:**1397–1404.
Kakizaki S, Yamamoto Y, Ueda A, Moore R, Sueyoshi T, and Negishi M (2003) Phenobarbital induction of drug/steroid-metabolizing enzymes and nuclear receptor CAR. *Biochim Biophys Acta* **1619:**239–242.
Kawamoto T, Kakizaki S, Yoshinari K, and Negishi M (2000) Estrogen activation of the nuclear orphan receptor CAR (constitutive active receptor) in induction of the mouse Cyp2b10 gene. *Mol Endocrinol* **14:**1897–1905.
Kawamoto T, Sueyoshi T, Zelko I, Moore R, Washburn K, and Negishi M (1999) Phenobarbital-responsive nuclear translocation of the receptor CAR in induction of the CYP2B gene. *Mol Cell Biol* **19:**6318–6322.
Kawana K, Ikuta T, Kobayashi Y, Gotoh O, Takeda K, and Kawajiri K (2003) Molecular mechanism of nuclear translocation of an orphan nuclear receptor, SXR. *Mol Pharmacol* **63:**524–531.
Kobayashi K, Sueyoshi T, Inoue K, Moore R, and Negishi M (2003) Cytoplasmic accumulation of the nuclear receptor CAR by a tetratricopeptide repeat protein in HepG2 cells. *Mol Pharmacol* **64:**1069–1075.
Kodama S, Koike C, Negishi M, and Yamamoto Y (2004) Nuclear receptors CAR and PXR cross talk with FOXO1 to regulate genes that encode drug-metabolizing and gluconeogenic enzymes. *Mol Cell Biol* **24:**7931–7940.
Koike C, Moore R, and Negishi M (2005) Localization of the nuclear receptor CAR at the cell membrane of mouse liver. *FEBS Lett* **579:**6733–6736.
Koike C, Moore R, and Negishi M (2007) Extracellular signal-regulated kinase is an endogenous signal retaining the nuclear constitutive active/androstane receptor (CAR) in the cytoplasm of mouse primary hepatocytes. *Mol Pharmacol* **71:**1217–1221.
Qatanani M and Moore DD (2005) CAR, the continuously advancing receptor, in drug metabolism and disease. *Curr Drug Metab* **6:**329–339.
Rosenfeld JM, Vargas R, Jr., Xie W, and Evans RM (2003) Genetic profiling defines the xenobiotic gene network controlled by the nuclear receptor pregnane X receptor. *Mol Endocrinol* **17:**1268–1282.
Skinner JA and Saltiel AR (2001) Cloning and identification of MYPT3: a prenylatable myosin targetting subunit of protein phosphatase 1. *Biochem J* **356:**257–267.
Squires EJ, Sueyoshi T, and Negishi M (2004) Cytoplasmic localization of pregnane X receptor and ligand-dependent nuclear translocation in mouse liver. *J Biol Chem* **279:**49307–49314.
Sueyoshi T, Kawamoto T, Zelko I, Honkakoski P, and Negishi M (1999) The repressed nuclear receptor CAR responds to phenobarbital in activating the human CYP2B6 gene. *J Biol Chem* **274:**6043–6046.
Sueyoshi T, Moore R, Pascussi JM, and Negishi M (2002) Direct expression of fluorescent protein-tagged nuclear receptor CAR in mouse liver. *Methods Enzymol* **357:**205–213.
Swales K and Negishi M (2004) CAR, driving into the future. *Mol Endocrinol* **18:**1589–1598.
Tien ES, Matsui K, Moore R, and Negishi M (2007) The nuclear receptor constitutively active/androstane receptor regulates type 1 deiodinase and thyroid hormone activity in the regenerating mouse liver. *J Pharmacol Exp Ther* **320:**307–313.
Tien ES and Negishi M (2006) Nuclear receptors CAR and PXR in the regulation of hepatic metabolism. *Xenobiotica* **36:**1152–1163.
Timsit YE and Negishi M (2007) CAR and PXR: the xenobiotic-sensing receptors. *Steroids* **72:**231–246.
Ueda A, Hamadeh HK, Webb HK, Yamamoto Y, Sueyoshi T, Afshari CA, Lehmann JM, and Negishi M (2002) Diverse roles of the nuclear orphan receptor CAR in regulating hepatic genes in response to phenobarbital. *Mol Pharmacol* **61:**1–6.
Vereshchagina N, Bennett D, Szoor B, Kirchner J, Gross S, Vissi E, White-Cooper H, and Alphey L (2004) The essential role of PP1beta in Drosophila is to regulate nonmuscle myosin. *Mol Biol Cell* **15:**4395–4405.
Wang H, Faucette S, Moore R, Sueyoshi T, Negishi M, and LeCluyse E (2004) Human constitutive androstane receptor mediates induction of CYP2B6 gene expression by phenytoin. *J Biol Chem* **279:**29295–29301.
Wei P, Zhang J, Egan-Hafley M, Liang S, and Moore DD (2000) The nuclear receptor CAR mediates specific xenobiotic induction of drug metabolism. *Nature* **407:**920–923.
Willson TM and Kliewer SA (2002) PXR, CAR and drug metabolism. *Nat Rev Drug Discov* **1:**259–266.
Xia J and Kemper B (2005) Structural determinants of constitutive androstane receptor required for its glucocorticoid receptor interacting protein-1-mediated nuclear accumulation. *J Biol Chem* **280:**7285–7293.
Xie W and Evans RM (2001) Orphan nuclear receptors: the exotics of xenobiotics. *J Biol Chem* **276:**37739–37742.
Xu RX, Lambert MH, Wisely BB, Warren EN, Weinert EE, Waitt GM, Williams JD, Collins JL, Moore LB, Willson TM, et al. (2004) A structural basis for constitutive activity in the human CAR/RXRalpha heterodimer. *Mol Cell* **16:**919–928.
Yamamoto Y, Kawamoto T, and Negishi M (2003) The role of the nuclear receptor CAR as a coordinate regulator of hepatic gene expression in defense against chemical toxicity. *Arch Biochem Biophys* **409:**207–211.
Yamamoto Y, Moore R, Goldsworthy TL, Negishi M, and Maronpot RR (2004) The orphan nuclear receptor constitutive active/androstane receptor is essential for liver tumor promotion by phenobarbital in mice. *Cancer Res* **64:**7197–7200.
Yamazaki Y, Kakizaki S, Horiguchi N, Sohara N, Sato K, Takagi H, Mori M, and Negishi M (2007) The role of the nuclear receptor constitutive androstane receptor in the pathogenesis of non-alcoholic steatohepatitis. *Gut* **56:**565–574.
Yong J, Tan I, Lim L, and Leung T (2006) Phosphorylation of myosin phosphatase targeting subunit 3 (MYPT3) and regulation of protein phosphatase 1 by protein kinase A. *J Biol Chem* **281:**31202–31211.
Yoshinari K, Kobayashi K, Moore R, Kawamoto T, and Negishi M (2003) Identification of the nuclear receptor CAR:HSP90 complex in mouse liver and recruitment of protein phosphatase 2A in response to phenobarbital. *FEBS Lett* **548:**17–20.
Zelko I, Sueyoshi T, Kawamoto T, Moore R, and Negishi M (2001) The peptide near the C terminus regulates receptor CAR nuclear translocation induced by xenochemicals in mouse liver. *Mol Cell Biol* **21:**2838–2846.

Address correspondence to: Dr. Tatsuya Sueyoshi, Pharmacogenetics section, Laboratory of Reproductive and Developmental Toxicology, National Institute of Environmental Health Sciences, National Institutes of Health, Research Triangle Park, NC 27709. E-mail: sueyoshi@niehs.nih.gov